

RESEARCH ARTICLE

An Active Fault Detection for Unmanned Surface Vehicles With Minor Fault

ZHI-HAO LIU¹, JIAN-NING LI², (Member, IEEE), WAN-YING YANG²,
MEI-YAN SHEN³, XU-FENG SHEN³, AND YANG LUO³

¹School of HDU-ITMO, Joint Institute, Hangzhou Dianzi University, Hangzhou 310018, China

²School of Automation, Hangzhou Dianzi University, Hangzhou 310018, China

³Hangzhou Qianhang Shipyard Company Ltd., Hangzhou 311256, China

Corresponding author: Jian-Ning Li (ljn@hdu.edu.cn)

This work was supported in part by the Zhejiang Provincial Natural Science Foundation of China under Grant LZ22F030008, in part by the National Natural Science Foundation of China under Grant 61733009, and in part by the Fundamental Research Funds for the Provincial Universities of Zhejiang under Grant GK229909299001-012.

ABSTRACT This article proposes an active fault detection method for Unmanned Surface Vehicles (USVs) with uncertain bounded disturbance to achieve the minor faults detection of USV. In practice, minor faults are the early cases of normal faults with the characteristic of low amplitude and difficulty to detection. At first, a set-membership estimation approach is used to describe the area topology of the nominal model of USVs and the fault models. Then, an auxiliary input signal is designed to enhance the character of minor faults, and the minor faults can be separated from the considered USVs in spite of uncertain bounded disturbances. Next, the considered problem is transformed into a nonconvex optimization problem, and the optimal auxiliary signal is obtained via solving the mixed integer quadratic programming (MIQP). Finally, a case study of the USVs is used to show the effectiveness of the proposed method.


INDEX TERMS Unmanned surface vehicles, active fault detection, set membership estimation, minor faults.

I. INTRODUCTION

In recent years, with the rapid development of technologies such as automatic control, the Internet of things, and big data, the level of unmanned equipment has been continuously improved. The research on unmanned ships has become an active field due to the large space for exploration and the effective practical use of unmanned ships. Unmanned surface vehicle (USV) has significant advantages because it is easy to deploy and operate in a variety of environments, so it is widely used in civil and military fields [1]. An overview of the application of USV by [2], describes that USV can be used for military mine clearance, anti-terrorism, anti-submarine, sea investigation, civil surveying and mapping, hydrology, environmental protection, and other tasks. In the process of the closed-loop system's execution, if there is a fault existing in some parts of USV, which will lead to the dynamic characteristics of the considered system may be reduced, even the abnormal operation of the whole system and huge

economic losses when it stops running. Therefore, the timely fault detection of USV can ensure the stability of the whole system and is of great significance to prevent the occurrence of major accidents.

Fault detection plays a vital role in the industrial process. In the past few decades, many authors have analyzed fault detection [3], [4], [5]. Fault detection methods can generally be divided into two categories: active fault detection [6], [7] and passive fault detection [8]. Most of the existing fault detection methods are carried out under the "passive" framework. By detecting the input and output signals of the system, without applying additional input signals to the system, the monitored behavior is compared with the normal behavior to confirm whether a malfunction occurs. Passive fault detection can be classified into two categories, one is based on qualitative analysis methods, such as expert systems, graph theory, etc [9]; The other is based on quantitative analysis methods, such as state estimation under redundant models [10], [11], parameter estimation [12], data-driven machine learning [13], [14], multiple statistical analysis [15] and information fusion. Passive fault detection methods like

The associate editor coordinating the review of this manuscript and approving it for publication was Guillermo Valencia-Palomo .

this do not impose additional input signals on the system so that they do not affect the evolution of the system, but at the same time, there is a lot of redundancy, which limits the ability to detect faults. Therefore, most of the existing fault detection applications in the USV direction are significant faults, but the significant faults in USV are all converted from minor faults. The so-called minor fault refers to a type of fault or anomaly that has a small amplitude, changes in an early stage, and changes slowly. Since a minor fault has a minimal impact on the operation of the system and is not easy to be detected, if the minor fault can be monitored in time, it can effectively avoid the adverse effect on the system after the increase of the fault, and ensure the stability of the system. This is also one of the research purposes of this article.

Compared with the significant fault detection based on a large number of researches, the detection of minor faults has only attracted attention in recent years. When a minor fault occurs, the characterization of the system is almost the same as that of the normal system; Therefore, in order to be more to ensure the safety of the system to a large extent, researchers have proposed many fault detection methods with minor faults as the detection target. In [16], for the early detection of minor faults in linear systems with unknown disturbances, a comprehensive adaptive sliding mode observer method was proposed, so that the observer can estimate minor faults and has strong robustness to unknown disturbances. In recent years, scholars have proposed an active fault detection method. Its working principle is as follows: under the condition of not affecting the normal operation of the system, minor fault detection is performed by injecting auxiliary signals, which is a new type of fault detection method with higher accuracy. For sensor faults in closed-loop systems, literature [17] proposed an online detection and estimation method for minor faults based on Kullback-Leibler (KL) distance. For the detection of small changes in the parameters of linear uncertain systems, a method to construct an optimal input signal to ensure a given detection accuracy is proposed by [12]. However, the active fault detection of the USV, which requires high safety, is almost blank. This is also the second motivation of this article.

This paper studies the minor fault detection of USV. The main contributions of this article are as follows:

a) To achieve the purpose of detecting the minor faults in the USV system, an active fault detection method is provided to design an auxiliary signal to strengthen the characterization of the minor fault in the USV.

b) By using the principle of set membership estimation, the modeling of USV is transformed into the zonotopic set, and the auxiliary signal which can improve the performance of minor fault detection is designed by the zonotopic active fault detection method.

The rest of this article is as follows. First, in Section 2, some preliminary introductions to the problem model and formula of USV are explained. Then in Section 3, the set of fully symmetric multicellular bodies output by the system is obtained through set membership estimation. Section 4 uses

the output set in the third section to get the optimal auxiliary separation signal. Section 5 carries on the simulation of USV. Finally, the summary of this article is introduced in Section 6.

II. MODEL DESCRIPTION AND PRELIMINARIES

A. MODEL DESCRIPTION

Generally, the motion of the USV in six degrees of freedom includes sway, yaw, roll, surge, heave, and pitch as following

$$\begin{cases} (m + m_x)\dot{u} - (m + m_y)vr = X \\ (m + m_y)\dot{u} + (m + m_x)ur = Y \\ (m + m_z)\dot{w} = Z \\ (I_{xx} + J_{xx})\dot{p} = K \\ (I_{yy} + J_{yy})\dot{q} = M \\ (I_{zz} + J_{zz})\dot{r} = N \end{cases} \quad (1)$$

u , v and w are the velocities of the USV in the direction of x , y and z . p , q and r are the angular velocities of the USV on the x , y and z axes, respectively. X , Y , and Z represent the sum of all forces in that direction. K , M and N represent the sum of all the moments on the corresponding axis. m , m_x , m_y and m_z represent ship mass and additional mass in their respective directions, respectively. I_{xx} , I_{yy} , and I_{zz} indicate the moment of the USV on the x , y and z axes. J_{xx} , J_{yy} , and J_{zz} represent the additional torque on each axis. The equation of the coordinate origin should be set in the center line of the ship. In addition, the equations of speed and ship steering motion are based on the following assumptions [18]:

- Homogeneous mass distribution and xz -plane symmetry.
- The heave and pitch motions can be neglected.
- The speed of the ship is constant.

Based on the assumption that the value of surge motion as velocity motion is constant, the additional torque of the ship is defined as zero. The USV equations of motion can be expressed as:

$$\begin{cases} m_y \frac{d^2 y}{dt^2} = Y, \text{ sway} \\ I_{zz} \frac{d^2 \psi}{dt^2} = N, \text{ yaw} \\ I_{xx} \frac{d^2 \phi}{dt^2} = K, \text{ roll} \end{cases} \quad (2)$$

x , y and z represent the vertical axis (backward and forward), the horizontal axis (to the right) and the vertical axis (from top to bottom); m_y respectively represent the effective mass of the ship in the y direction; y , ψ and ϕ represents directional distance, heading angle and roll angle.

The response model of USV maneuvering motion is adopted in this paper. The rudder angle is taken as the input of the system, the yaw angle, and the roll angle as the output of the system, and the whole ship is regarded as a dynamic system. The model used in this paper has been proved to be feasible by [19] through experiments. The output and the transfer function of the output are represented by the Laplace transform. For the yaw motion, it can be expressed by a first-order response model after simplification in the

frequency domain, just like the Nomoto model [18], the response equation is as follows:

$$\psi(s) = \frac{K}{s(1 + T_s)}\delta(s) \quad (3)$$

For the rolling motion equation, the disturbance in the motion is modeled by the second-order transfer function driven by white noise in the frequency domain [20]. After simplification, we can get the following transfer function:

$$\phi(s) = \frac{\omega_n^2}{s^2 + 2\zeta\omega_n + \omega_n^2}\delta(s) \quad (4)$$

In addition, combined with (3) and (4) and the USV coordinate system is shown in Fig 1. The motion parameters of the unmanned ship are described in the table 1.

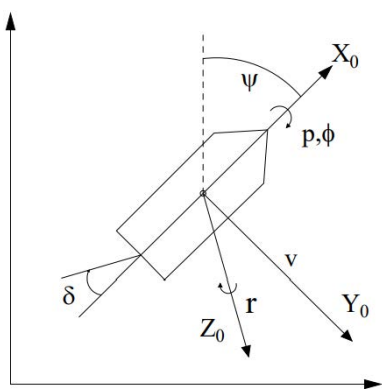


FIGURE 1. Motion coordinate system for USV.

TABLE 1. Description of motion parameters of unmanned ship.

DOF	Force/moment	Linear/Angular velocity	Position/angle
Surge	X	u	x
Sway	Y	v	y
Heave	Z	w	z
Roll	K	p	phi
Pitch	M	q	theta
Yaw	N	r	psi

Due to the interaction of roll, sway, and yaw motion, incorporate the influence of high-order disturbance. Ignoring some hydrodynamic effects, we can obtain the following motion transfer functions:

$$\begin{cases} v(s) = \frac{K_{dv}}{1 + T_v s} \delta(s) \\ \psi(s) = \frac{[K_{dr}\delta(s) + K_{vr}v(s) + \omega_\psi(s)]}{(1 + T_r s)s} \\ \phi(s) = \frac{\omega_n^2 [K_{dp}\delta(s) + K_{vp}v(s) + \omega_\phi(s)]}{s^2 + 2\zeta\omega_n s + \omega_n^2} \end{cases} \quad (5)$$

v, ψ, ϕ and δ represent the yaw speed, heading angle, roll angle and rudder angle caused by rudder motion; ω_ψ and ω_ϕ represent the influence of the wave on ψ and ϕ respectively; T_v and T_r represent the time constant of the transfer function,

$K_{vr}, K_{vp}, K_{dv}, K_{dr}$ and K_{dp} represent the known parameters; ζ and ω_n represent the damping ratio without damping and natural frequency. The specific meaning of the parameter is expressed by [21].

Due to the need of the algorithm in this paper, we convert formula (5) into the state space expression in time domain through Laplace inverse change. In order to deal with the higher-order terms contained in the formula (4), we convert the higher-order terms as follows.

$$\begin{cases} \dot{\psi}(t) = p(t) \\ \dot{\phi}(t) = r(t) \end{cases} \quad (6)$$

Combined with formula (5) and formula (6), we can obtain the state space expression of USV motion. The state-space model of the USV's sway, yaw, and roll motion states can be obtained:

$$\begin{cases} \dot{x}(t) = Ax(t) + B\delta(t) + E_1\omega(t) \\ y(t) = Cx(t) + De(t) \\ x(t_0) = x_0 \end{cases} \quad (7)$$

$x(t) = [v(t) \ r(t) \ \psi(t) \ p(t) \ \phi(t)]^T$ with $\delta(t) \in \mathbb{R}^m$ and $x(t) \in \mathbb{R}^n$, p and r denote the roll velocity and yaw velocity, $\omega(t) = [\omega_\psi(t) \ \omega_\phi(t)]^T$ means wave disturbance with $\omega(t) \in \mathbb{R}^p$, $e(t) \in \mathbb{R}^v$ is measurement noise and $x_0 \in \mathbb{R}^n$ denoting the initial instant. Moreover C is the observation matrix of appropriate dimension A, B and E are defined:

$$A = \begin{bmatrix} -\frac{1}{T_v} & 0 & 0 & 0 & 0 \\ \frac{K_{vr}}{T_r} & -\frac{1}{T_r} & 0 & 0 & 0 \\ 0 & 1 & 0 & 0 & 0 \\ \omega_n^2 K_{vp} & 0 & 0 & -2\zeta\omega_n & -\omega_n^2 \\ 0 & 0 & 0 & 1 & 0 \end{bmatrix}$$

$$B = \begin{bmatrix} \frac{K_{dv}}{T_v} \\ \frac{K_{dr}}{T_r} \\ 0 \\ \omega_n^2 K_{dp} \\ 0 \end{bmatrix}, \quad E = \begin{bmatrix} 0 & 0 \\ \frac{1}{T_r} & 0 \\ 0 & 0 \\ 0 & \omega_n^2 \\ 0 & 0 \end{bmatrix}, \quad D = I$$

Specifically, using Euler's approximation method. This method will produce bounded approximation errors. Due to the influence of set membership estimation theory and unknown but bounded disturbance, we add the error of Euler approximation directly to the bounded disturbance. According to the continuous formula (7). For a given sampling period t_s , a discrete model of the USV can be established:

$$\begin{cases} x_i(k+1) = A^{[i]}x_i(k) + B^{[i]}u(k) + E^{[i]}\omega(k) \\ y_i(k) = C^{[i]}x_i(k) + D^{[i]}e(k) \end{cases} \quad (8)$$

$i \in [1, 2, \dots, n]$. $i = 1$ represents the nominal system, $i = 2, 3, 4, \dots$ is the model with different minor faults, $x_i(k+1)$ and $y_i(k)$ represent the state value and output value of the system. $A^{[i]}, B^{[i]}$ and $C^{[i]}$ is state matrix, input matrix and output matrix, respectively. $D^{[i]}$ and $E^{[i]}$ represent disturbance coefficient matrix. sh_i is the active fault detection input signal to be designed later.

The minor faults on the USV are difficult to be detected due to disturbances and uncertain parameters, that is, the nominal model and the fault model can not be distinguished without the input of the designed auxiliary signal.

To increase the detectable range of minor faults, active fault detection methods are used for detection. By designing an auxiliary input signal, a brief detection is made in a simulation model of an USV (the parameters are obtained from the actual motion identification of the USV). The purpose of detection is to completely distinguish the matrix of different states and to judge whether the current USV state is in the fault state. And return the detection results to the console of the USV. The auxiliary separation signals are injected into the system to strengthen the characterization of system faults. The active fault detection method in this paper is based on the theory of zonotopic set membership estimation in order to achieve the purpose of separating the nominal system and the fault systems, that is

$$y_a \cap y_b = \emptyset, a \neq b, a, b \in \{1, 2, 3, \dots, n\}$$

where y_a and y_b are the output of different model.

In Fig 2, (a) represent the output set of the scenarios without auxiliary signal. Blue, red and green respectively represents the nominal state, fault 1 and fault 2, there is an intersection between them, and fault detection cannot be completely performed. (b) Represent the output set of the scenarios that input the auxiliary separation signal, in which the set of fault-free state and fault state is completely separated, and fault detection can be performed.

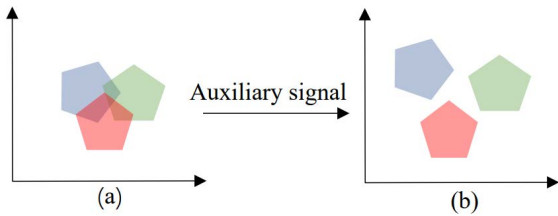


FIGURE 2. The process of fault detection.

B. PRELIMINARIES

This article uses the method of zonotopic set membership estimation to calculate. A zonotope is defined as:

$$T = \{L\xi + h : \xi \in \mathbb{R}^{n_s}, \|\xi\|_\infty \leq 1\} = L\xi \oplus h \quad (9)$$

$h \in \mathbb{R}^n$ is the center of T , $L = [l_1 l_2 l_3 \dots l_m] \in \mathbb{R}^{n \times m}$ is the generator matrix of T . Below we use $T = \{L, h\}$ to express (9).

The operations of zonotopes is define:

$$\begin{aligned} T_1 \oplus T_2 &= \{L_1, h_1\} \oplus \{L_2, h_2\} \\ &= \{(L_1 + L_2)\xi + (h_1 + h_2)\} \\ &= \{\{L_1 L_2\}, h_1 + h_2\} \\ MT &= M\{L\xi \oplus h\} \\ &= \{ML\xi + Mh : \xi \in \mathbb{R}^n, \|\xi\|_\infty < 1\} \end{aligned}$$

which M is multiplying matrix, T_1, T_2 is zonotopes.

Lemma 1 [22]: Let $A = \{L_A, c_a + d_a\}$ and $B = \{L_B, c_b + d_b\}$. then $A \cap B = \emptyset$ if and only if $c_a - c_b \notin \{L_a, d_a\} \oplus \{L_b, d_b\}$.

III. REACHABLE SET OF OUTPUT USING ZONOTOPIC SET-MEMBERSHIP

Define the auxiliary input signal $\tilde{u} = (u_0, \dots, u_{N-1}) \in \mathbb{R}^{Nn_u}$. For $0 \leq l \leq k < N$, we defined $\tilde{u}_{\ell:k} = (u_\ell, \dots, u_k)$. Similarly, $\tilde{i} = (i_0, \dots, i_N) \in \tilde{\mathbb{I}}$ indicates different fault models. x_0 represents the initial state matrix. The reachable set of state will be used to describe the separated input set below. $S_k(\tilde{u}, \tilde{i}, x_0, \tilde{w}, v)$ and $O_k(\tilde{u}, \tilde{i}, x_0, \tilde{w}, v)$ represent the state and output at time k . Let $S_{l:k}(\tilde{u}, \tilde{i}, x_0, \tilde{w}, v) = (S_l, \dots, S_k)$ and $O_{l:k}(\tilde{u}, \tilde{i}, x_0, \tilde{w}, v) = (O_l, \dots, O_k)$, then we can be derived that $(S_j, O_j) = (S_j, O_j)(\tilde{u}_{0:j-1}, \tilde{i}_{0:j}, x_0, \tilde{w}_{0:j-1}, v_j), l < j < k$.

Denote the matrices \tilde{A} and \tilde{B} , etc. Through the iteration of (8), which depend on l to k , such that:

$$\begin{aligned} S^{[l]}(\tilde{u}, \tilde{i}, x_0, \tilde{w}) &= \tilde{A}^{[l]}(\tilde{i})x_0 + \tilde{B}^{[l]}(\tilde{i})\tilde{u} + \tilde{E}^{[l]}(\tilde{i})\tilde{w} \\ O^{[l]}(\tilde{u}, \tilde{i}, x_0, \tilde{w}) &= \tilde{C}^{[l]}(\tilde{i})S(\tilde{u}, \tilde{i}, x_0, \tilde{w}) + \tilde{D}_v^{[l]}(\tilde{i})\tilde{v} \end{aligned} \quad (10)$$

where

$$\begin{aligned} \tilde{S}^{[l]} &= \begin{bmatrix} S_0^{[l]} \\ S_2^{[l]} \\ \vdots \\ S_{N-1}^{[l]} \end{bmatrix}, \tilde{O}^{[l]} = \begin{bmatrix} O_0^{[l]} \\ O_2^{[l]} \\ \vdots \\ O_{N-1}^{[l]} \end{bmatrix}, \tilde{w}^{[l]} = \begin{bmatrix} w_0^{[l]} \\ w_1^{[l]} \\ \vdots \\ w_{N-1}^{[l]} \end{bmatrix} \\ \tilde{u} &= \begin{bmatrix} u_0 \\ u_1 \\ \vdots \\ u_{N-1} \end{bmatrix}, \tilde{A}^{[l]} = \begin{bmatrix} A^{[l]0} \\ A^{[l]1} \\ \dots \\ A^{[l]N-1} \end{bmatrix} \\ \tilde{B}^{[l]} &= \begin{bmatrix} 0 & 0 & \dots & 0 \\ B^{[l]} & 0 & \dots & 0 \\ \vdots & & \ddots & \vdots \\ A^{[l]N-1} B^{[l]} & A^{[l]N-2} B^{[l]} & \dots & B^{[l]} \end{bmatrix} \\ \tilde{E}^{[l]} &= \begin{bmatrix} 0 & 0 & \dots & 0 \\ E^{[l]} & 0 & \dots & 0 \\ A^{[l]} E^{[l]} & E^{[l]} & \ddots & 0 \\ A^{[l]N-1} E^{[l]} & A^{[l]N-2} E^{[l]} & \dots & E^{[l]} \end{bmatrix} \\ \tilde{C}^{[l]} &= \begin{bmatrix} C^{[l]} & 0 \\ \vdots & \vdots \\ 0 & C^{[l]} \end{bmatrix} \\ \tilde{D}_v^{[l]} &= \begin{bmatrix} D_v^{[l]} & 0 \\ \vdots & \vdots \\ 0 & D_v^{[l]} \end{bmatrix} \end{aligned}$$

Using the operations of zonotopes, we can get

$$\begin{aligned} \mathbb{S}(\tilde{u}, \tilde{i}) &= \tilde{A}^{[l]}(\tilde{i})x_0 \oplus \tilde{B}^{[l]}(\tilde{i})\tilde{u} \oplus \tilde{E}^{[l]}(\tilde{i})\tilde{W} \\ \mathbb{O}(\tilde{u}, \tilde{i}) &= \tilde{C}^{[l]}(\tilde{i})\mathbb{S}(\tilde{u}, \tilde{i}, x_0, \tilde{w}) \oplus \tilde{D}_v^{[l]}(\tilde{i})\tilde{V} \end{aligned} \quad (11)$$

$X_0 = \{L_0, h_0\}$, $W = \{L_W, h_W\}$ and $V = \{L_V, h_V\}$, \tilde{W} is a zonotope that the center $\tilde{h}_w = (h_w, \dots, h_w)$ and the generator matrix $\tilde{L}_W = \text{diag}(L_W, \dots, L_W)$. \tilde{V} is the same as W . Let's replace (11) with another expression.

$$\begin{aligned} \mathbb{S}(\tilde{u}, \tilde{i}) &= \left\{ L^{\mathbb{S}}(\tilde{i}), \tilde{S}(\tilde{u}, \tilde{i}) \right\} \\ \mathbb{O}(\tilde{u}, \tilde{i}) &= \left\{ L^{\mathbb{O}}(\tilde{i}), \tilde{O}(\tilde{u}, \tilde{i}) \right\} \end{aligned} \quad (12)$$

With the centers $\tilde{S}(\tilde{u}, \tilde{i}) = \tilde{S}(\tilde{u}, \tilde{i}, h_0, h_{\tilde{W}}, h_{\tilde{V}})$ and $\tilde{O}(\tilde{u}, \tilde{i}) = \tilde{O}(\tilde{u}, \tilde{i}, h_0, h_{\tilde{W}}, h_{\tilde{V}})$. The generator matrixs $L^{\mathbb{S}}(\tilde{i}) = [\tilde{A}^{[i]}L_0 \tilde{E}^{[i]}L_{\tilde{W}}]$ and $L^{\mathbb{O}}(\tilde{i}) = [\tilde{C}^{[i]}(i)L^{\mathbb{S}}(\tilde{i}) \tilde{D}_v^{[i]}(i)L_V]$. Moreover, splitting the expression of zonotope for subsequent solutions $\tilde{S}_N(\tilde{u}, \tilde{i}) = \tilde{S}_N(0, \tilde{i}) + B_N^{\mathbb{S}}(\tilde{i})\tilde{u}$ and $\tilde{O}_N(\tilde{u}, \tilde{i}) = \tilde{O}_N(0, \tilde{i}) + B_N^{\mathbb{O}}(\tilde{i})\tilde{u}$, where $B_N^{\mathbb{S}}(\tilde{i})$ and $B_N^{\mathbb{O}}(\tilde{i})$ are the element of the Nth recursion.

$$B_{k+1}^{\mathbb{S}}(\tilde{i}) = [A(i_k)B_k^{\mathbb{S}} B(i_k)], \quad B_k^{\mathbb{O}}(\tilde{i}) = C(i_k)B_k^{\mathbb{S}} \quad (13)$$

IV. DESIGN FOR OPTIMAL AUXILIARY SEPARATION SIGNAL

This section, using the above output set to design the auxiliary optimal separation signal, Assuming that the initial auxiliary separation signal injected is $\tilde{u} = [u_0, u_1, u_2 \dots u_{N-1}]$, and the output $\tilde{y} = [y_0, y_1, y_2 \dots y_{N-1}]$ is observed. And define $J(\tilde{\mathbf{u}}) = \sum_{k=0}^{N-1} (u_k)^T R(u_k)$.

Definition 1 [22]: For different scenarios $i \in \mathbb{I}$, there are different \tilde{y} corresponding to i .

$$\tilde{y} \in \tilde{\mathbb{O}}(\tilde{u}, \tilde{i}) \quad (14)$$

Our purpose is to ensure that for each \tilde{y} only represents one type of i , scenario \mathbb{I} includes different faults already nominal system.

Definition 2 [23]: $\tilde{u} \in R^{Nn_u}$ is a separate auxiliary signal, if and only if

$$\tilde{\mathbb{O}}(\tilde{u}, \tilde{i}) \cap \tilde{\mathbb{O}}(\tilde{u}, \tilde{j}) = \emptyset \quad (15)$$

Analogously, \tilde{u} is a separating input which can separates \mathbb{I} in $[0, N]$, if it separates every $i, j \in \mathbb{I}$, and $i \neq j$.

Theorem 1: For system (8), the set of separated auxiliary signals \tilde{u} is

$$\tilde{\Omega} = \{\tilde{u} : \Delta \tilde{Z}^{[i,j]}\tilde{u} \notin \tilde{N}(i, j)\} \quad (16)$$

where, $\forall i, j \in \mathbb{I}, i \neq j, \tilde{N}(i, j) = \{[L_N^{\mathbb{O}}(\tilde{i})L_N^{\mathbb{O}}(\tilde{j}), O_N(0, \tilde{i}) - O_N(0, \tilde{j})]\}$ and $\Delta \tilde{Z}^{[i,j]} = (\tilde{C}(i)\tilde{B}(i) - \tilde{C}(j)\tilde{B}(j))$.

Proof: Through (13), we can describe the expression (15)

$$\left\{ L^{\mathbb{O}}(\tilde{i}), \tilde{O}_N(0, \tilde{i}) + B_N^{\mathbb{O}}(\tilde{i})\tilde{u} \right\} \cap \left\{ L^{\mathbb{O}}(\tilde{j}), \tilde{O}_N(0, \tilde{j}) + B_N^{\mathbb{O}}(\tilde{j})\tilde{u} \right\}$$

Using Lemma1, we can get Theorem 1.

In this paper, by applying the auxiliary input signal to the actual simulation model of USV, the final fault detection effect is obtained and returned to the console of USV. The performance index of the auxiliary input signal is mainly the size of the signal input, and the larger signal will lead to an increase in detection time, so on the premise that minor faults

can be detected, the size of the auxiliary signal can be reduced as much as possible. So we transform the signal design problem into the Mixed Integer Quadratic Programming (MIQP) problem. This kind of method is used to solve the MIP model with quadratic objectives but no quadratic constraints.

We can describe the MIQP problem as follows:

$$\begin{aligned} \min_{\tilde{u}_k} & \tilde{u}_k^T R \tilde{u}_k \\ \text{s.t.} & \mathbb{O}_N^{[i]} \cap \mathbb{O}_N^{[j]} = \emptyset, i \neq j, i, j \in \{0, 1, 2, 3 \dots p\} \end{aligned} \quad (17)$$

In order to facilitate the calculation below, we make some simplifications $\Delta \tilde{Z}^{[i,j]} = \Delta \tilde{Z}^{[p]}$, $\tilde{N}(i, j) = \tilde{N}^{[p]} = \{L^{[p]}, h^{[p]}\}$ which $p \in \{1, \dots, \mathbb{I}\}$ express different scenarios and matrix L is row full rank.

Theorem 2: For each \tilde{u} and $p \in \{1, \dots, \mathbb{I}\}$

$$\begin{aligned} \inf_{\tilde{u} \in U} & \tilde{u}^T R \tilde{u} \\ \hat{\delta}^{[p]}(\tilde{u}) & \equiv \min \delta^{[p]} \\ \text{s.t.} & Z^{[p]}\tilde{u} = L^{[p]}\xi^{[p]} + h^{[p]}, \xi^{[p]}_{\infty} \leq 1 + \delta^{[p]} \\ & \tilde{Z}^{[p]}\tilde{u} \notin \tilde{N}^{[p]} \text{ if and only if } \hat{\delta}^{[p]}(\tilde{u}) > 0 \end{aligned} \quad (18)$$

Proof: $L^{[p]}$ is full rank, (18) is reasonable. If $\tilde{Z}^{[p]}\tilde{u} \notin \tilde{N}^{[p]}$, then $\tilde{Z}^{[p]}\tilde{u}$ makes $\|\xi^{[p]}\|_{\infty} \leq 1$ and $Z^{[p]}\tilde{u} = L^{[p]}\xi^{[p]} + h^{[p]}$. Therefore, $\delta^{[p]} \leq 0$ has no feasible solution, which means $\hat{\delta}^{[p]}(\tilde{u}) > 0$. On the contrary, if $\hat{\delta}^{[p]}(\tilde{u}) > 0$, then (15) has no reasonable point when $\delta^{[p]} \leq 0$ is satisfied. This means that $\tilde{Z}^{[p]}\tilde{u}$ makes $\|\xi^{[p]}\|_{\infty} \leq 1$ and $Z^{[p]}\tilde{u} = L^{[p]}\xi^{[p]} + h^{[p]}$, so $\tilde{Z}^{[p]}\tilde{u} \notin \tilde{N}^{[p]}$. Then we can get Theorem2.

The design of the optimal auxiliary separation signal can be solved by MIQP problem. then we will give condition as follow.

Theorem 3: For $\forall \tilde{u} \in \tilde{U}$ where $\tilde{U} = U \times U \dots \times U$ as the auxiliary separation signal sets can write (18) as

$$\begin{aligned} \inf_{\tilde{u} \in U} & \tilde{u}^T R \tilde{u} \\ \text{s.t.} & \varepsilon \leq \hat{\delta}^{[p]}(\tilde{u}) \leq \hat{\delta}_m^{[p]}, \forall p \in \{1, \dots, \mathbb{I}\} \end{aligned} \quad (19)$$

A single-level plan can be obtained by replacing the linear internal plan in (18), using the necessary and sufficient conditions for optimality, and the conditions are as follows:

$$\inf_{\tilde{u}} \tilde{u}^T R \tilde{u} \quad (20)$$

$$\min \left\{ J(\tilde{\mathbf{u}}) : \tilde{\mathbf{u}} \in \tilde{U}, \varepsilon \leq \hat{\delta}^{[p]}(\tilde{\mathbf{u}}) \leq \hat{\delta}_m^{[p]}, p = 1, \dots, \mathbb{I} \right\} \quad (21)$$

$$\tilde{Z}^{[p]}\tilde{\mathbf{u}} = L^{[p]}\xi^{[p]} + h^{[p]} \quad (22)$$

$$\xi^{[p]}_{\infty} \leq 1 + \delta^{[p]} \quad (23)$$

$$\left(L^{[p]} \right)^T \lambda^{[p]} = \left(\mu_1^{[p]} - \mu_2^{[p]} \right) \quad (24)$$

$$1 = \left(\mu_1^{[p]} + \mu_2^{[p]} \right)^T \mathbf{1} \quad (25)$$

$$\mathbf{0} \leq \mu_1^{[p]}, \mu_2^{[p]} \quad (26)$$

$$0 = \mu_{1,k}^{[p]} \left(\xi_k^{[p]} - 1 - \delta^{[p]} \right), \quad \forall k = 1, \dots, n_g^{[p]} \quad (27)$$

$$0 = \mu_{2,k}^{[p]} \left(\xi_k^{[p]} + 1 + \delta^{[p]} \right), \quad \forall k = 1, \dots, n_g^{[p]} \quad (28)$$

where $\lambda^{[p]}$, $\mu_1^{[p]}$ and $\mu_2^{[p]}$ are lagrange multiplier, 1 is a unit vector, $q_1^{[p]}$, $q_2^{[p]}$ are binary variables. The feasible set represented by $\hat{\delta}^{[p]}(\tilde{u}) > 0$ may not be a union, and there may be no lower bound to satisfy it, so constraint $\varepsilon \leq \hat{\delta}^{[p]}(\tilde{u})$ is used. Where $\varepsilon > 0$ is the minimum threshold that satisfies the separation condition. And assume that $\hat{\delta}_m^{[p]} > 1$. the feasible set in (19) is not closed For each p , $\varepsilon \leq \hat{\delta}^{[p]}(\tilde{u}) \leq \hat{\delta}_m^{[p]}$, $p = 1, \dots, \mathbb{I}$ (22) to (28) can be used instead. $\mu_{1,k}$ and $\mu_{2,k}$ satisfy.

$$\begin{aligned} \mu_1^{[ij]} &= \left[\mu_{1,1}^{[ij]} \mu_{1,2}^{[ij]} \dots \mu_{1,2s_y}^{[ij]} \right]^T \in \mathbb{R}^{2s_y} \\ \mu_2^{[ij]} &= \left[\mu_{2,1}^{[ij]} \mu_{2,2}^{[ij]} \dots \mu_{2,2s}^{[ij]} \right]^T \in \mathbb{R}^{2s_y} \end{aligned} \quad (29)$$

Proof: The feasible set represented by (18) may not be a closed set, there may be no lower bound to satisfy. So the constraint $\hat{\delta}^{[p]}(\tilde{u}) > \varepsilon$ is used, where $\varepsilon > 0$ represents the minimum threshold required to satisfy the separation condition, such as $\hat{\delta}^{[p]}\tilde{u} < \delta_m^{[p]}$. Besides, the lagrangian equation for optimal problem (19) is:

$$\begin{aligned} \mathcal{L} &= \delta^{[p]} + \lambda^{[p]} \left(L^{[p]} \xi^{[p]} + h^{[p]} - \tilde{Z}^{[p]} \tilde{u} \right) \\ &+ \mu_{1,1}^{[p]} \left(-\xi_1^{[p]} - 1 - \delta^{[p]} \right) + \mu_{1,2}^{[p]} \left(-\xi_2^{[p]} - 1 - \delta^{[p]} \right) \\ &+ \dots + \mu_{2,2s_y}^{[p]} \left(-\xi_{2s_y}^{[p]} - 1 - \delta^{[p]} \right) \\ &+ \mu_{1,1}^{[p]} \left(\xi_1^{[p]} - 1 - \delta^{[p]} \right) + \mu_{2,2}^{[p]} \left(\xi_2^{[p]} - 1 - \delta^{[p]} \right) \\ &+ \dots + \mu_{2,2s_y}^{[p]} \left(\xi_{2s_y}^{[p]} - 1 - \delta^{[p]} \right) \\ &= \delta^{[p]} + \lambda^{[p]} \left(L^{[p]} \xi^{[p]} + h^{[p]} - \tilde{Z}^{[p]} \tilde{u} \right) \\ &- \left(\mu_1^{[p]} \right)^T \xi^{[p]} - \left(\mu_1^{[p]} \right)^T 1 - \left(\mu_1^{[p]} \right)^T 1 \delta^{[p]} \\ &+ \left(\mu_2^{[p]} \right)^T \xi^{[p]} - \left(\mu_2^{[p]} \right)^T 1 - \left(\mu_2^{[p]} \right)^T 1 \delta^{[p]} \end{aligned} \quad (30)$$

We can get the first-order optimal condition through the derivation of (29).

$$\begin{aligned} \frac{\partial \mathcal{L}}{\partial \delta^{[q]}} &= 1 - \left(\mu_1^{[q]} + \mu_2^{[q]} \right)^T 1 = 0 \\ \frac{\partial \mathcal{L}}{\partial \delta^{[ij]}} &= \left(L^{[q]} \right)^T - \mu_1^{[q]} + \mu_2^{[q]} = 0 \\ \mu_{1,l}^{[q]} \left(\xi_l^{[q]} - 1 - \delta^{[q]} \right) &= 0 \\ \mu_{2,l}^{[q]} \left(\xi_l^{[q]} + 1 + \delta^{[q]} \right) &= 0 \end{aligned} \quad (31)$$

Complementarity constraints (27) and (28) are non-convex, we use binary variables $p_1^{[q]}$, $p_2^{[q]}$ instead of expression and get the following formula:

$$\begin{aligned} q_{1,k}^{[p]} &= 1 \mu_{1,k}^{[p]} \text{free}, \left(\xi_k^{[p]} - 1 - \delta^{[p]} \right) = 0 \\ q_{1,k}^{[p]} &= 0 \mu_{1,k}^{[p]} = 0, \left(\xi_k^{[p]} - 1 - \delta^{[p]} \right) \text{free} \\ q_{2,k}^{[p]} &= 1 \mu_{2,k}^{[p]} \text{free}, \left(\xi_k^{[p]} + 1 + \delta^{[p]} \right) = 0 \\ q_{2,k}^{[p]} &= 0 \mu_{2,k}^{[p]} = 0 \left(\xi_k^{[p]} + 1 + \delta^{[p]} \right) \text{free} \end{aligned} \quad (32)$$

Replace the formula (31) by the formula (23) (25) (26) to get:

$$\begin{aligned} \mu_{1,k}^{[p]} &\leq q_{1,k}^{[p]}, \quad \mu_{2,k}^{[p]} \leq q_{2,k}^{[p]} \\ \left(\xi_k^{[p]} - 1 - \delta^{[p]} \right) &\in \left[-2 \left(1 + \hat{\delta}_m^{[p]} \right) \left(1 - q_{1,k}^{[p]} \right), 0 \right] \\ \left(\xi_k^{[p]} + 1 + \delta^{[p]} \right) &\in \left[0, 2 \left(1 + \hat{\delta}_m^{[p]} \right) \left(1 - q_{2,k}^{[p]} \right) \right] \end{aligned} \quad (33)$$

Therefore, the signal solution process can be rewritten as

$$\begin{aligned} \min_{\tilde{u}, \delta} [p], \xi^{[p]}, \lambda^{[p]}, \mu_1^{[p]}, \mu_2^{[p]}, q_1^{[p]}, q_2^{[p]} J(\tilde{u}) \\ \text{s.t. } \tilde{u} \in \tilde{U} \\ \left\{ \begin{aligned} \varepsilon \leq \delta^{[p]} \leq \delta_m^{[p]}, (22) - (28) \\ q_1^{[p]}, q_2^{[p]} \in \{0, 1\}^{n_s^g}, (33) \end{aligned} \right\} \quad \forall p \in \{1, \dots, \mathbb{I}\} \end{aligned} \quad (34)$$

Then Theorem 3 is obtained by proof. This is a MIQP problem that can be solved using the tool CPLEX in matlab.

Finally, algorithm 1 is obtained to solve the problem of minor fault detection in USV, such as Algorithm 1.

Algorithm 1 Active Minor Fault Detection for USV

- 1: Get the zonotope state expression of USV.
 - 2: Given $A^{[i]}$, $B^{[i]}$, $C^{[i]}$, $E^{[i]}$ and $D^{[i]}$, $i = 1, 2, \dots, \mathbb{I}$.
 - 3: Calculate L and \bar{O} without auxiliary input signal
 - 4: **for** $k = 1$ to **end do**
 - 5: Obtain \tilde{u}_{k-1} by Theorem 3, than inject it in system;
 - 6: Calculate L and \bar{O} according to (11);
 - 7: **end for**
 - 8: Describe the health output zonotope set $\mathbb{O}^{[1]}$ and the faulty output zonotope set $\mathbb{O}^{[i]}$;
 - 9: **if** $y_k \in \mathbb{O}^{[1]}$ **then**
 - 10: Fault detection result is 0, the system is health;
 - 11: **else if** $y_k \in \mathbb{O}^{[i]}$, $i = 1.2 \dots I$ **then**
 - 12: Fault detection result is 1, the system exist fault;
 - 13: **else if** $y_k \notin \mathbb{O}^{[i]}$, $i = 0.1.2 \dots I$ **then**
 - 14: Fault detection result is -1, can't judge whether the system is faulty.
 - 15: **end if**
-

V. SIMULATION

To verify the effectiveness of the optimal auxiliary signal design method, this chapter conducts simulation experiments for USV without auxiliary signal and auxiliary signal.

First of all, through [20], we get the nominal model of the USV and the state parameters of the USV under different faults as shown in Table 2, set Sampling time $t_s = 0.1s$ Describe and calculate each fault mode.

The model 1 represents health system with matrices A_1 , B_1 , E_1 and C_1 in formula (8), choose the parameter as

$$A^{[1]} = \begin{bmatrix} -1.9000 & 0 & 0 & 0 & 0 \\ -1.0925 & -2.3750 & 0 & 0 & 0 \\ 0 & 1.0000 & 0 & 0 & 0 \\ 2.1202 & 0 & 0 & -6.7839 & -2.4679 \\ 0 & 0 & 0 & 1.0000 & 0 \end{bmatrix}$$

TABLE 2. Parameters of USV.

MODEL	T_v	T_r	K_{vr}	K_{vp}	K_{dv}	K_{dr}	K_{dp}	ζ	ω_n
1	0.5263	0.4211	-0.4600	0.7980	0.0380	-0.0103	-0.0202	2.0840	1.63
2	0.4211	0.4474	-0.5100	0.7890	0.1900	-0.0152	-0.0217	2.0840	1.63
3	0.6053	0.5000	-0.3500	0.3800	0.0384	-0.0106	-0.0203	2.0840	1.63
4	0.6053	0.4474	-0.5300	0.7890	0.0228	-0.0019	-0.0058	2.0840	1.63
5	0.4737	0.3947	-0.7000	1.2160	0.0380	-0.0106	-0.0202	2.0840	1.63

$$B^{[1]} = \begin{bmatrix} 0.0722 \\ -0.0244 \\ 0 \\ -0.0537 \\ 0 \end{bmatrix} \quad E^{[1]} = \begin{bmatrix} 0 & 0 \\ 2.3750 & 0 \\ 0 & 0 \\ 0 & 2.6569 \\ 0 & 0 \end{bmatrix}$$

$$C^{[1]} = [1 \ 0.8 \ 1 \ -1 \ 0.6]$$

Model 2 represents a minor fault in the potentiometer of the steering gear. This fault will lead to a rudder impact. Make the rudder angle rotate too fast. This fault will make the state parameter K_{dv} larger. Over time, the steering gear may be damaged and the steering gear may fail. The specific parameters of the fault model can be seen from Table 2.

$$A^{[2]} = \begin{bmatrix} -2.3750 & 0 & 0 & 0 & 0 \\ -1.1400 & -2.2353 & 0 & 0 & 0 \\ 0 & 1.0000 & 0 & 0 & 0 \\ 2.1202 & 0 & 0 & -6.6738 & -2.6569 \\ 0 & 0 & 0 & 1.0000 & 0 \end{bmatrix}$$

$$B^{[2]} = \begin{bmatrix} 0.4513 \\ -0.0340 \\ 0 \\ -0.5750 \\ 0 \end{bmatrix} \quad E^{[2]} = \begin{bmatrix} 0 & 0 \\ 2.2353 & 0 \\ 0 & 0 \\ 0 & 2.2569 \\ 0 & 0 \end{bmatrix}$$

$$C^{[2]} = [1 \ 0.8 \ 1 \ -1 \ 0.6]$$

Model 3 indicates the minor fault of the anti-rolling rudder in the rudder-rolling stabilization system so that the anti-rolling rudder does not achieve the desired effect. Parameter K_{vp} decreases, and the specific parameters are shown in Table 2. With time, the rudder anti-rolling may have a significant fault of aggravated rolling, which needs to be detected in time. The state expression of the fault is as follows:

$$A^{[3]} = \begin{bmatrix} -1.6522 & 0 & 0 & 0 & 0 \\ -0.7000 & -2.000 & 0 & 0 & 0 \\ 0 & 1.0000 & 0 & 0 & 0 \\ 1.0096 & 0 & 0 & -6.7638 & -2.3759 \\ 0 & 0 & 0 & 1.0000 & 0 \end{bmatrix}$$

$$B^{[3]} = \begin{bmatrix} 0.0634 \\ -0.213 \\ 0 \\ -0.0537 \\ 0 \end{bmatrix} \quad E^{[3]} = \begin{bmatrix} 0 & 0 \\ 2.3750 & 0 \\ 0 & 0 \\ 0 & 2.3759 \\ 0 & 0 \end{bmatrix}$$

$$C^{[3]} = [1 \ 0.8 \ 1 \ -1 \ 0.6]$$

Model 4 represents the minor fault of the voltage instability of the steering gear, which hinders the rotation of the rudder

blade. This reduces the parameters K_{dr} and K_{dp} . The parameters of the fault model are shown in Table 2, and the state expression of the fault is as follows:

$$A^{[4]} = \begin{bmatrix} -1.6522 & 0 & 0 & 0 & 0 \\ -1.1847 & -2.2353 & 0 & 0 & 0 \\ 0 & 1.0000 & 0 & 0 & 0 \\ 2.1202 & 0 & 0 & -6.7938 & -2.6569 \\ 0 & 0 & 0 & 1.0000 & 0 \end{bmatrix}$$

$$B^{[4]} = \begin{bmatrix} 0.0377 \\ -0.0042 \\ 0 \\ -0.0153 \\ 0 \end{bmatrix} \quad E^{[4]} = \begin{bmatrix} 0 & 0 \\ 2.2353 & 0 \\ 0 & 0 \\ 0 & 2.6569 \\ 0 & 0 \end{bmatrix}$$

$$C^{[4]} = [1 \ 0.8 \ 1 \ -1 \ 0.6]$$

Model 5 shows that there is a slight wear on the rudder blade of the steering gear, so that the USV can not reach the expected first angle. It results in the increase of parameters K_{vr} and K_{vp} , as shown in Table 2. With the passage of time, the rudder blade will break and need to be detected in time. The state expression of the fault is as follows:

$$A^{[5]} = \begin{bmatrix} -2.1111 & 0 & 0 & 0 & 0 \\ -1.7733 & -2.5333 & 0 & 0 & 0 \\ 0 & 1.0000 & 0 & 0 & 0 \\ 3.2308 & 0 & 0 & -6.7938 & -2.6569 \\ 0 & 0 & 0 & 1.0000 & 0 \end{bmatrix}$$

$$B^{[5]} = \begin{bmatrix} 0.0802 \\ -0.0270 \\ 0 \\ -0.0537 \\ 0 \end{bmatrix} \quad E^{[5]} = \begin{bmatrix} 0 & 0 \\ 2.5333 & 0 \\ 0 & 0 \\ 0 & 2.6569 \\ 0 & 0 \end{bmatrix}$$

$$C^{[5]} = [1 \ 0.8 \ 1 \ -1 \ 0.6]$$

Through Algorithm 1, we get the zonotopes' L and \bar{O} without auxiliary separation signal in different situations.

Finally we denote it as Figure 3.

In generator notation, define $X_0 = \{0.2I, (-3, -3)\}$, $W = \{0.5I, 0\}$ and $V = \{0.2, 0\}$.

Fig 3 shows the nominal and faulty output groups without using auxiliary separation signals. In this figure, zonotopes with different colors are the output sets of the nominal model and different faulty models. When the auxiliary input signal is not injected into the system, the output set is the intersection of the output set of the nominal model and the faulty model. When the output set crosses, it is unable to determine whether the system is currently malfunctioning or distinguish the type

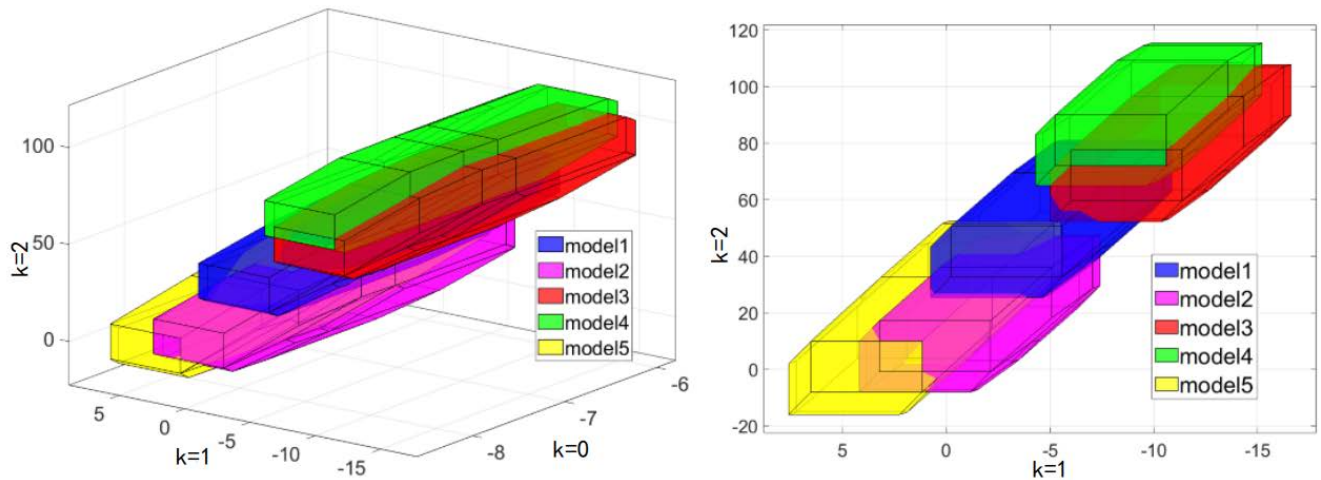


FIGURE 3. The output set for scenarios without auxiliary separation signal.

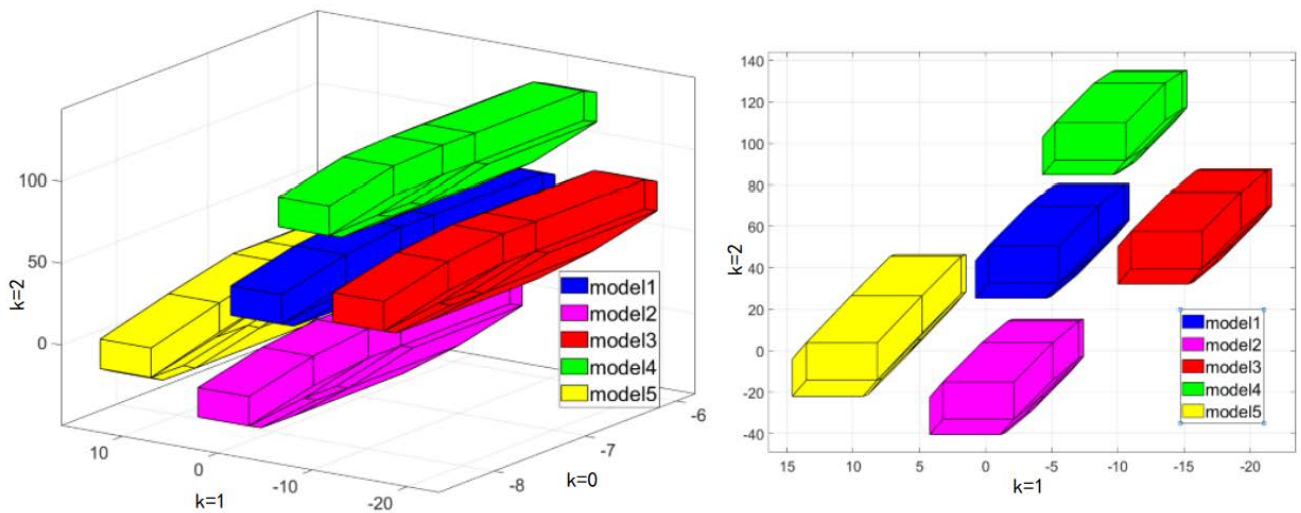


FIGURE 4. The output set for scenarios with auxiliary separation signal.

of faults. For example, fault model 2 and fault model 5 are the factors that affect the stability of the ship. It can not be well distinguished when there is no auxiliary signal input. Therefore, to diagnose minor faults in the system, and separate different types of faults, we need to inject excitation signals into the system to strengthen system characterization for detection.

Then we will get the optimal auxiliary separation signal according to Theorem 3, we can get the optimal auxiliary separation signal. Inject the signal into the detection system. The injection of the auxiliary signal will not affect the generation matrix of zonotope, so we get the \bar{O} of zonotope below. Finally we can get Fig 3.

In Fig 4, we design the auxiliary signal input through algorithm 1 of this paper and inject the signal into the detection system. We get that the five zonopotes sets in Fig 3 have no intersection, achieve complete separation, and get the result

we expected. Among the minor faults we define, there are fault states that are difficult to distinguish. The existence of these faults may affect the safety of the USV in the future. By injecting auxiliary signals, first, we can completely distinguish different fault states and find the exact fault point. Second, we can completely distinguish between the healthy state and the minor fault state and detect the existence of the minor fault in time to prevent the minor fault from turning into a significant fault. Achieved the purpose of active fault detection of USV.

The simulated system experiment will be carried out, and the operating conditions of the system as follow:

$$Actual\ system \begin{cases} Health\ status & 0 < k < 3 \\ Fault\ model\ 5 & 4 < k < 6 \end{cases} \quad (35)$$

Through formula 8 and algorithm, we can get the final output and auxiliary signal.

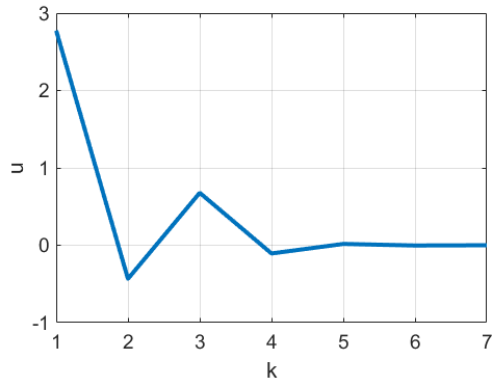


FIGURE 5. The amplitude of auxiliary input signal for zonotope framework.

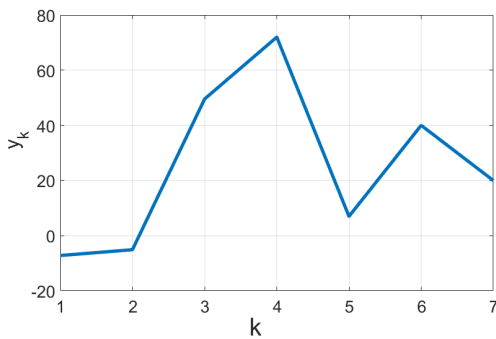


FIGURE 6. Output Y_k of unmanned ship under set conditions.

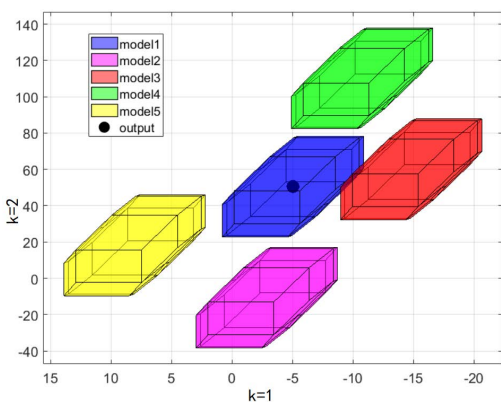


FIGURE 7. The simulation result of output zonotope at $k \in [1, 2]$.

The simulation results of output zonotopes in areb with $k \in [5, 6]$ shown in Fig 7. As can be seen from the figure, the output of the actual system is in a normal state.

As shown in Fig 8, when $k \in [5, 6]$, the output of the system is included in the set of fault 5, so it is judged to be fault 5.

Combining Fig 3, Fig 4 and simulation experiments. First of all, we apply the set membership estimation to the fault detection method of the USV. Through Fig 4, we can know that there is an intersection between the different minor fault models and the health model. this makes it difficult for us

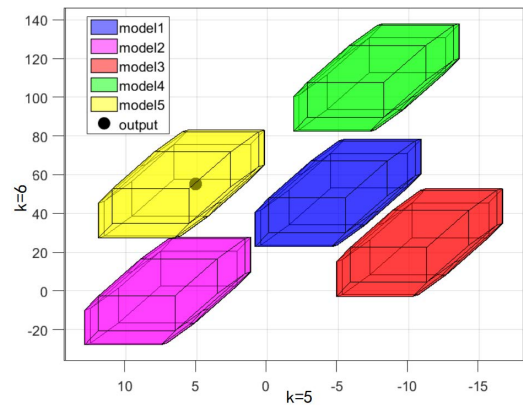


FIGURE 8. The simulation result of output zonotope at $k \in [5, 6]$.

to judge whether there is a minor fault and the location of the fault in a short time. In this case, we inject the auxiliary signal obtained by Algorithm 1 into the system and we can get Fig 4. In Fig 4, we make a complete distinction between health models and different micro models. We can diagnose minor faults and determine the location of faults, thus reflecting the superiority of active fault detection.

VI. CONCLUSION

Aiming at various minor fault detection problems of USV, this paper designs a zonotope active fault detection method and considers the uncertainty of the USV system. The zonotope model of USV is obtained through the equation of motion of USV, and each matrix is derived. The problem of active fault detection and optimization separation is further transformed into a MIQP problem to solve. A suitable auxiliary signal is injected into the system to amplify the fault characteristics of the system without affecting the stability of the system, to achieve the purpose of fault detection. Finally, the simulation experiment of USV shows the rationality of the method.

REFERENCES

- [1] Y. Ma, Z. Nie, S. Hu, Z. Li, and M. Sotelo, "Fault detection filter and controller co-design for unmanned surface vehicles under dos attacks," *IEEE Trans. Intell. Transp. Syst.*, vol. 22, no. 99, pp. 1–13, Feb. 2020.
- [2] R. Yan, P. Shuo, S. Hanbing, and P. Yongjie, "The development and mission of unmanned surface vehicles," *J. Mar. Sci. Appl.*, vol. 9, no. 4, pp. 451–457, 2010.
- [3] Q. Zhang and S. Geng, "Dynamic uncertain causality graph applied to dynamic fault diagnoses of large and complex systems," *IEEE Trans. Rel.*, vol. 64, no. 3, pp. 910–927, Apr. 2015.
- [4] F. Xu, J. Tan, X. Wang, V. Puig, B. Liang, B. Yuan, and H. Liu, "Generalized set-theoretic unknown input observer for LPV systems with application to state estimation and robust fault detection," *Int. J. Robust Nonlinear Control*, vol. 27, no. 17, pp. 3812–3832, Nov. 2017.
- [5] Y. Wang, V. Puig, and G. Cembrano, "Robust fault estimation based on zonotopic Kalman filter for discrete-time descriptor systems," *Int. J. Robust Nonlinear Control*, vol. 28, no. 16, pp. 5071–5086, Nov. 2018.
- [6] R. Nikoukhah, S. L. Campbell, and K. Drake, "An active approach for detection of incipient faults," *Int. J. Syst. Sci.*, vol. 41, no. 2, pp. 241–257, Feb. 2010.
- [7] H. Niemann, "A setup for active fault diagnosis," *IEEE Trans. Autom. Control*, vol. 51, no. 9, pp. 1572–1578, Sep. 2006.

- [8] X. Li and F. Zhu, "Fault-tolerant control for Markovian jump systems with general uncertain transition rates against simultaneous actuator and sensor faults," *Int. J. Robust Nonlinear Control*, vol. 27, pp. 1572–1578, Dec. 2017.
- [9] M. Simandl, J. Skach, and I. Puncochár, "Approximation methods for optimal active fault detection," in *Proc. IEEE Int. Conf. Control Autom.*, Jun. 2014, pp. 103–108.
- [10] M. Pourasghar, V. Puig, and C. Ocampo-Martinez, "Interval observer versus set-membership approaches for fault detection in uncertain systems using zonotopes," *Int. J. Robust Nonlinear Control*, vol. 29, no. 10, pp. 2819–2843, Jul. 2019.
- [11] H. Wang, "Fault detection for output feedback control systems with actuator stuck faults: A steady-state-based approach," *Int. J. Robust Nonlinear Control*, vol. 29, pp. 2819–2843, Oct. 2019.
- [12] R. Nikoukhah and S. L. Campbell, "On the detection of small parameter variations in linear uncertain systems," *Eur. J. Control*, vol. 14, no. 2, pp. 158–171, Jan. 2008.
- [13] M. Kallas, G. Mourou, D. Maquin, and J. Ragot, "Data-driven approach for fault detection and isolation in nonlinear system," *Int. J. Adapt. Control Signal Process.*, vol. 32, no. 11, pp. 1569–1590, Nov. 2018.
- [14] B. Cai, Y. Zhao, H. Liu, and M. Xie, "A data-driven fault diagnosis methodology in three-phase inverters for PMSM drive systems," *IEEE Trans. Power Electron.*, vol. 32, no. 7, pp. 5590–5600, Jul. 2017.
- [15] G. Cirrincione, H. Henao, M. Delgado, and J. A. Ortega, "Bearing fault diagnosis by EXIN CCA," in *Proc. Int. Joint Conf. Neural Netw. (IJCNN)*, Jun. 2012, pp. 1–7.
- [16] C. Liu, B. Jiang, K. Zhang, and Y. K. Wu, "Incipient fault detection of linear system with disturbance," *J. Shanghai Jiaotong Univ.*, vol. 49, no. 6, pp. 889–896, 2015.
- [17] S. Tao, Y. Chai, and Y. Wang, "Micro-fault diagnosis of closed-loop system sensor based on Kullback–Leibler distance," *IET Control Theory Appl.*, vol. 36, no. 6, pp. 909–914, 2019.
- [18] T. I. Fossen, *Guidance Control of Ocean Vehicles*. Hoboken, NJ, USA: Wiley, 1994.
- [19] J. Van Amerongen, P. G. M. Van Der Klugt, and H. R. Van Nauta Lemke, "Rudder roll stabilization for ships," *Automatica*, vol. 26, no. 4, pp. 679–690, Jul. 1990.
- [20] S. Saelid, N. Jenssen, and J. Balchen, "Design and analysis of a dynamic positioning system based on Kalman filtering and optimal control," *IEEE Trans. Autom. Control*, vol. AC-28, no. 3, pp. 331–339, Mar. 1983.
- [21] P. Klugt, *Rudder Roll Stabilization*. Delft, The Netherlands: Delft Univ. of Technology, 1987.
- [22] J. K. Scott, R. Findeisen, R. D. Braatz, and D. M. Raimondo, "Input design for guaranteed fault diagnosis using zonotopes," *Automatica*, vol. 50, no. 6, pp. 1580–1589, Jun. 2014.
- [23] J. Wang, Y. Shi, M. Zhou, Y. Wang, and V. Puig, "Active fault detection based on set-membership approach for uncertain discrete-time systems," *Int. J. Robust Nonlinear Control*, vol. 30, no. 14, pp. 5322–5340, Sep. 2020.



JIAN-NING LI (Member, IEEE) received the Ph.D. degree in control science and engineering from Zhejiang University, Hangzhou, China, in 2013.

He is currently an Associate Professor with the School of Automation, Hangzhou Dianzi University, Hangzhou. In 2012, he was a Visiting Scholar with the Department of Mechanical Engineering, Dalhousie University, Halifax, NS, Canada. From 2018 to 2019, he was a Visiting Scholar with the Department of Electrical and Computer Engineering, University of California at Riverside, Riverside, CA, USA. His research interests include fault-tolerant control, robust control, multiagent systems, and networked control systems.



WAN-YING YANG received the B.E. degree from the Jiangsu University of Science and Technology, Zhejiang, China, in 2021. She is currently pursuing the master's degree with Hangzhou Dianzi University, Hangzhou, China.

Her research interests include teleoperation systems and fault-tolerant control.



MEI-YAN SHEN was born in Wuhu, Anhui, China, in 1982. She is currently the Deputy General Manager of Hangzhou Qianhang Shipyard Company Ltd. Her research interest includes ship management.



XU-FENG SHEN was born in Wuhu, Anhui, China, in 1986. He received the B.E. degree in electronic science and technology and the joint M.Sc. degree in industry and business administration from the China University of Mining and Technology, Beijing, China, in 2008, and The Open University of Hong Kong, Hong Kong, China, in 2018. He is currently the Deputy General Manager and a Legal Representative at Hangzhou Qianhang Shipyard Company Ltd. His research

interest includes ship control and production.



ZHI-HAO LIU received the B.E. degree from the Zhejiang University of Water Resources and Electric Power, Zhejiang, China, in 2020. He is currently pursuing the master's degree with Hangzhou Dianzi University, Hangzhou, China.

His research interests include fault diagnosis and fault-tolerant control.



YANG LUO was born in Chongqing, China, in 1977. He received the B.E. degree in ship electrification from the Zhejiang University of Technology, Zhejiang, China, in 2008. He is currently the General Manager of Hangzhou Qianhang Shipyard Company Ltd. His research interests include ship control, production, and management.

...